Table 3. Number and location of tumors in offspring treated with $MnCl_2 4H_2O$ for 34 weeks

Group	No. of offspring	Brain	Spinal cord	Cranial nerves	Peri-pheral nerves	Extra-neural[a]	Nega-tive
Male							
Control	21	13	4	4	3	12	2
0.002% $MnCl_2$	21	12	4	9	3	13	0
0.01% $MnCl_2$	20	11	2	6	3	14	1
0.05% $MnCl_2$	18	12	3	4	3	16	0
Female							
Control	19	12	4	6	3	4	1
0.002% $MnCl_2$	24	18	4	6	4	7	3
0.01% $MnCl_2$	26	16	3	5	3	4	5
0.05% $MnCl_2$	24	13	3	4	0	6	5

a, including adenoma and adenocarcinoma in lung, adenoma and nephroblastoma in kidney, C-cell adenoma and follucular cell adenoma in thyroid and adenoma in mammary gland..

Table 4. The incidence of non-neural tumors in offspring treated with $MnCl_2$ $4H_2O$ for 34 weeks

Group	No. of offspring	Lung		Kidney		Thyroid		Mammary gland
		Ad	Ac	Ad	Nb	C-cell Ad	Follicular cell Ad	Ad
Male								
Control	21	9	4	0	0	0	0	0
0.002% $MnCl_2$	21	12	4	0	1	0	0	0
0.01% $MnCl_2$	20	12	7	0	0	0	0	0
0.05% $MnCl_2$	18	13	10	0	0	0	0	0
Female								
Control	19	2	0	1	0	0	0	0
0.002% $MnCl_2$	24	6	1	0	0	0	0	0
0.01% $MnCl_2$	26	2	0	1	0	1	0	0
0.05% $MnCl_2$	24	3	0	0	1	0	1	1

Ad, Adenoma
Ac, Adenocarcinoma
Nb, Nephroblastoma

Table 5. Water consumption and nicotine intake of dams treated with test chemicals for 3 weeks after ENU administration

Group	No. of dams	Water consumption (g/rat/day)	Nicotine intake (mg/kg b.w./day)
Control	5	58.0	0
Nicotine 0.002%	5	41.7	1.6
Nicotine 0.01%	5	28.3	6.0
Nicotine 0.025–0.05%	5	7.0	5.1
Propane sultone 0.04%	5	45.4	–

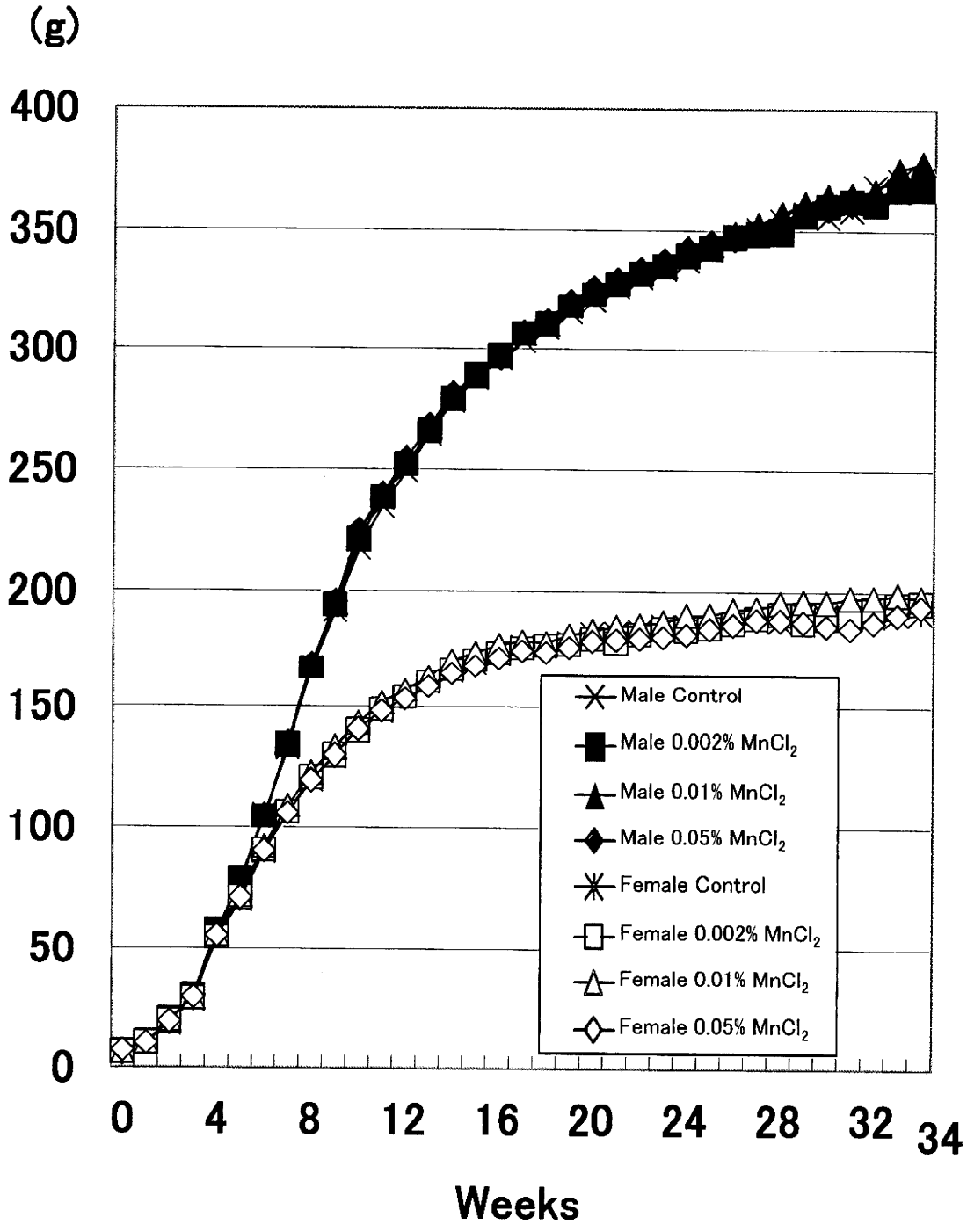

Figure 3. Body weight curves of offspring treated with $MnCl_2$ $4H_2O$ for 34 weeks

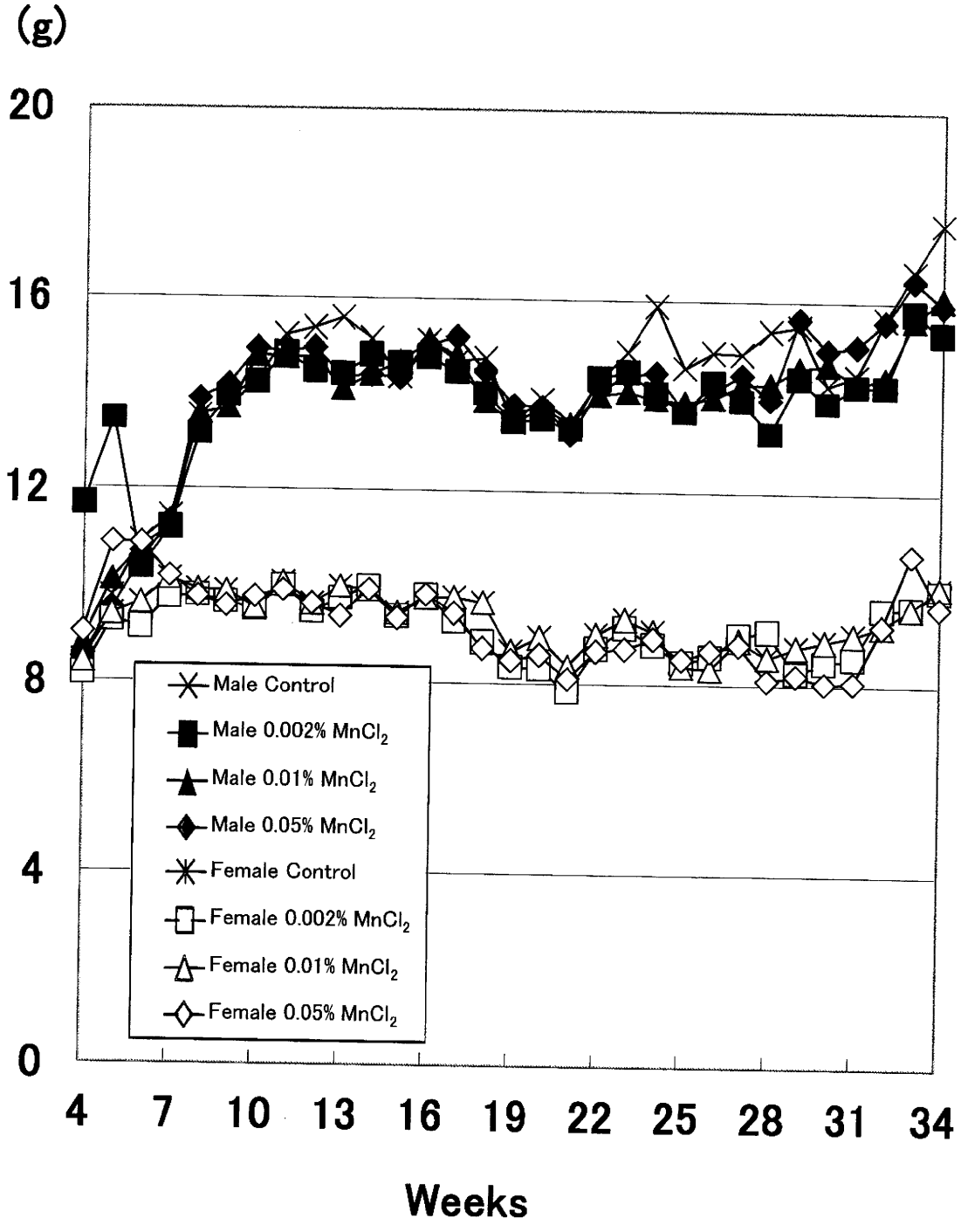

Figure 4. Food consumption of offspring treated with $MnCl_2\ 4H_2O$ for 34 weeks

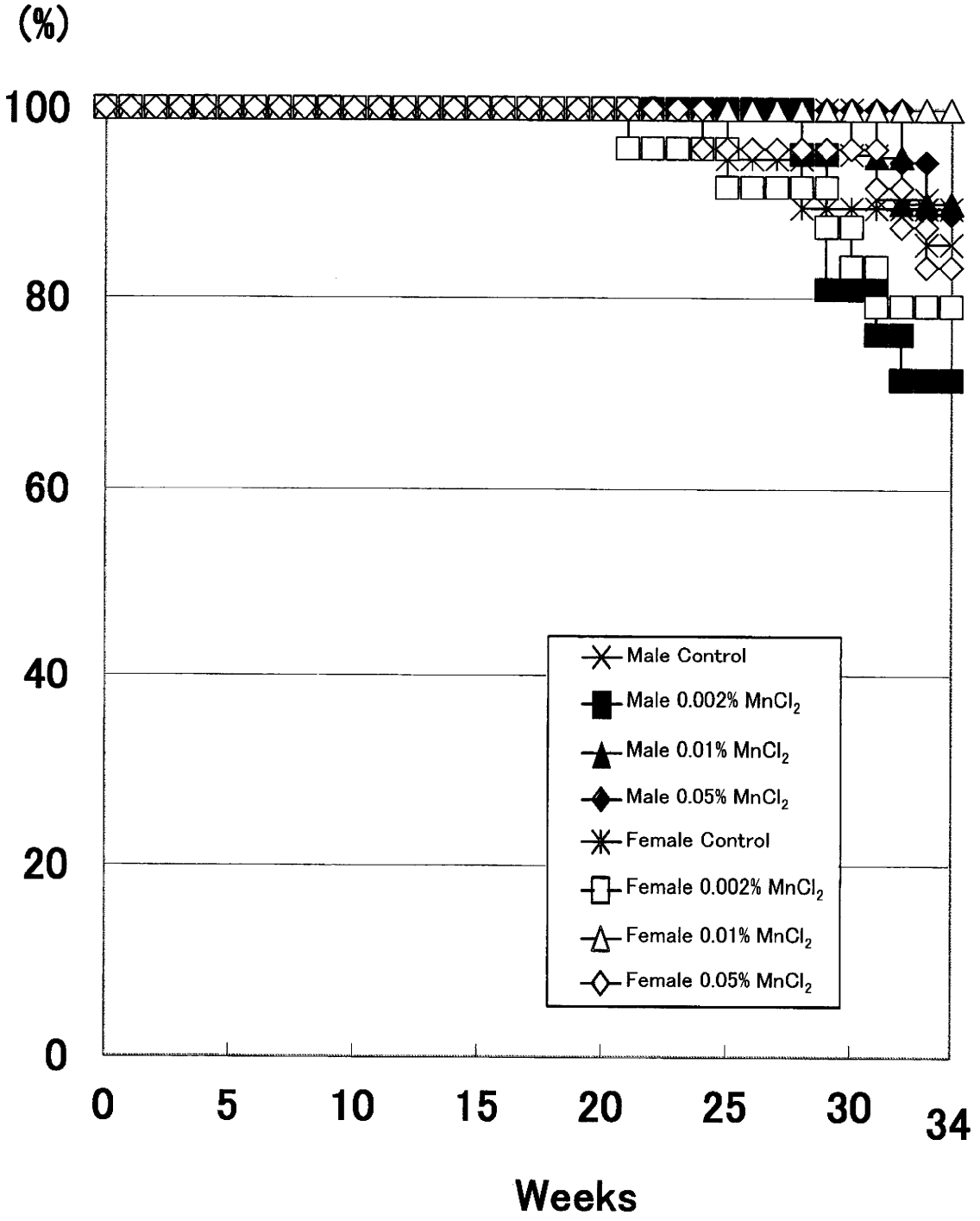

Figure 5. Survival curves of offspring treated with $MnCl_2\,4H_2O$ for 34 weeks

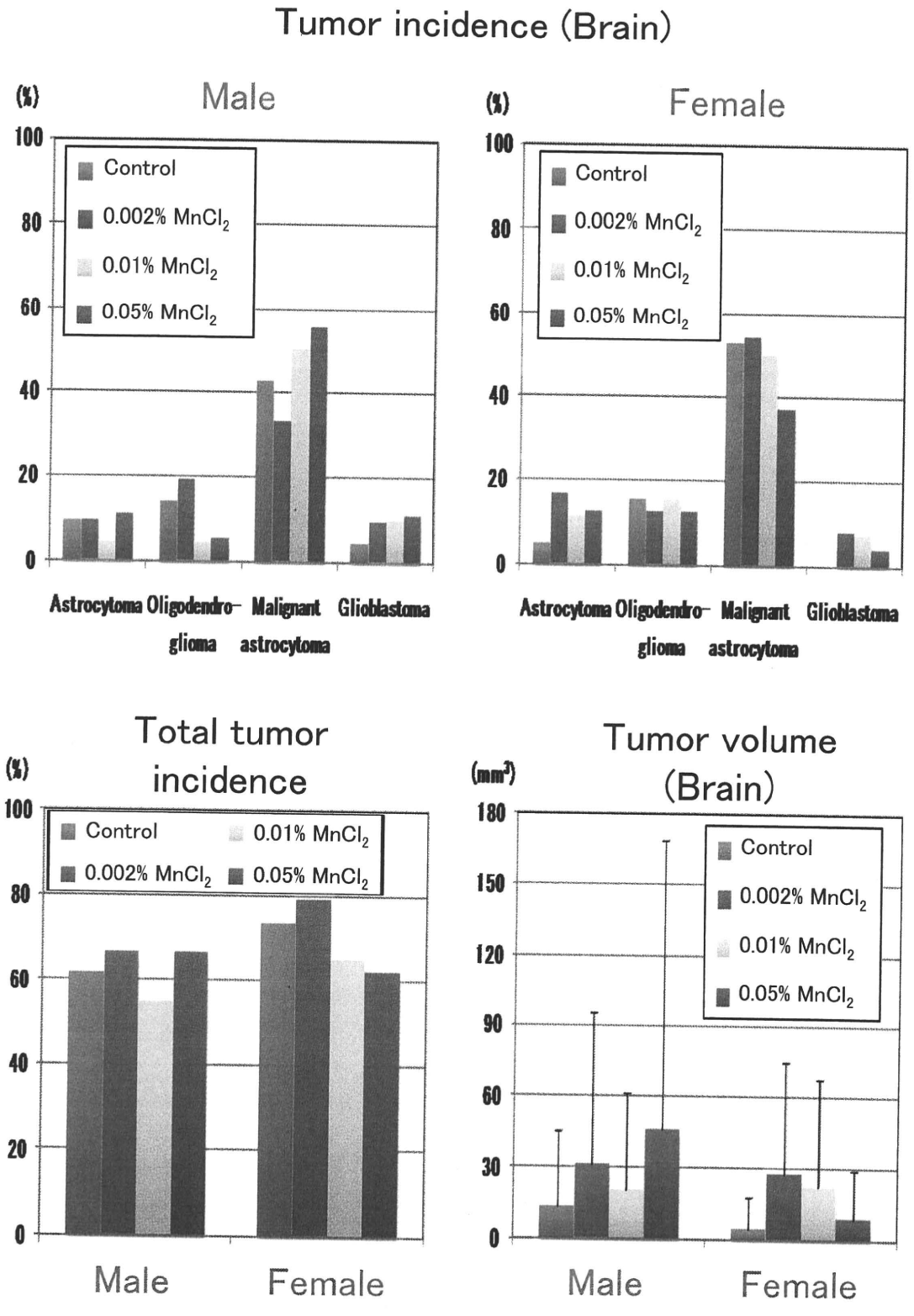

Figure 6. The incidence and volume of central nervous system tumors in offspring treated with $MnCl_2\ 4H_2O$ for 34 weeks

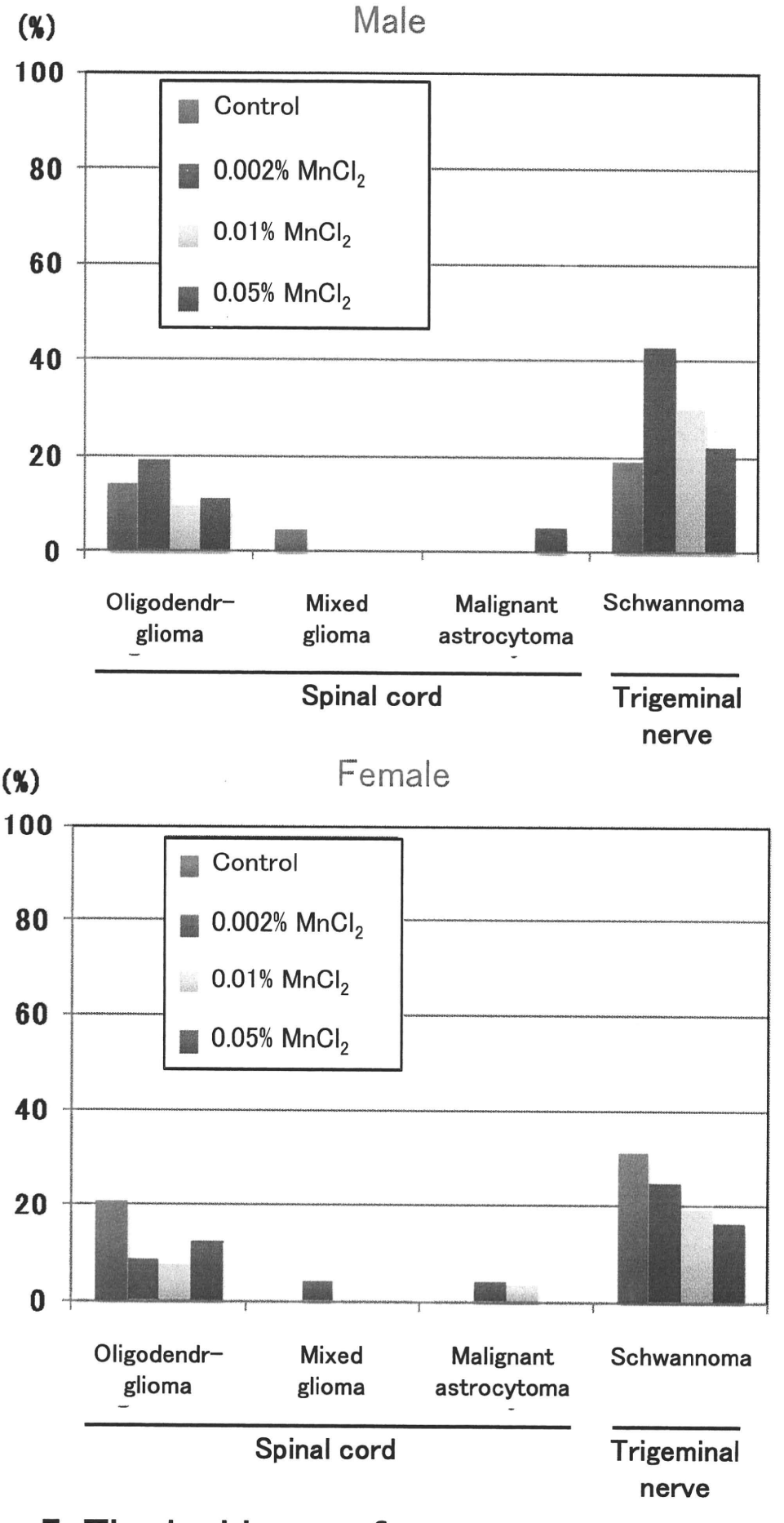

Figure 7. The incidence of nervous system tumors in offspring treated with $MnCl_2\,4H_2O$ for 34 weeks

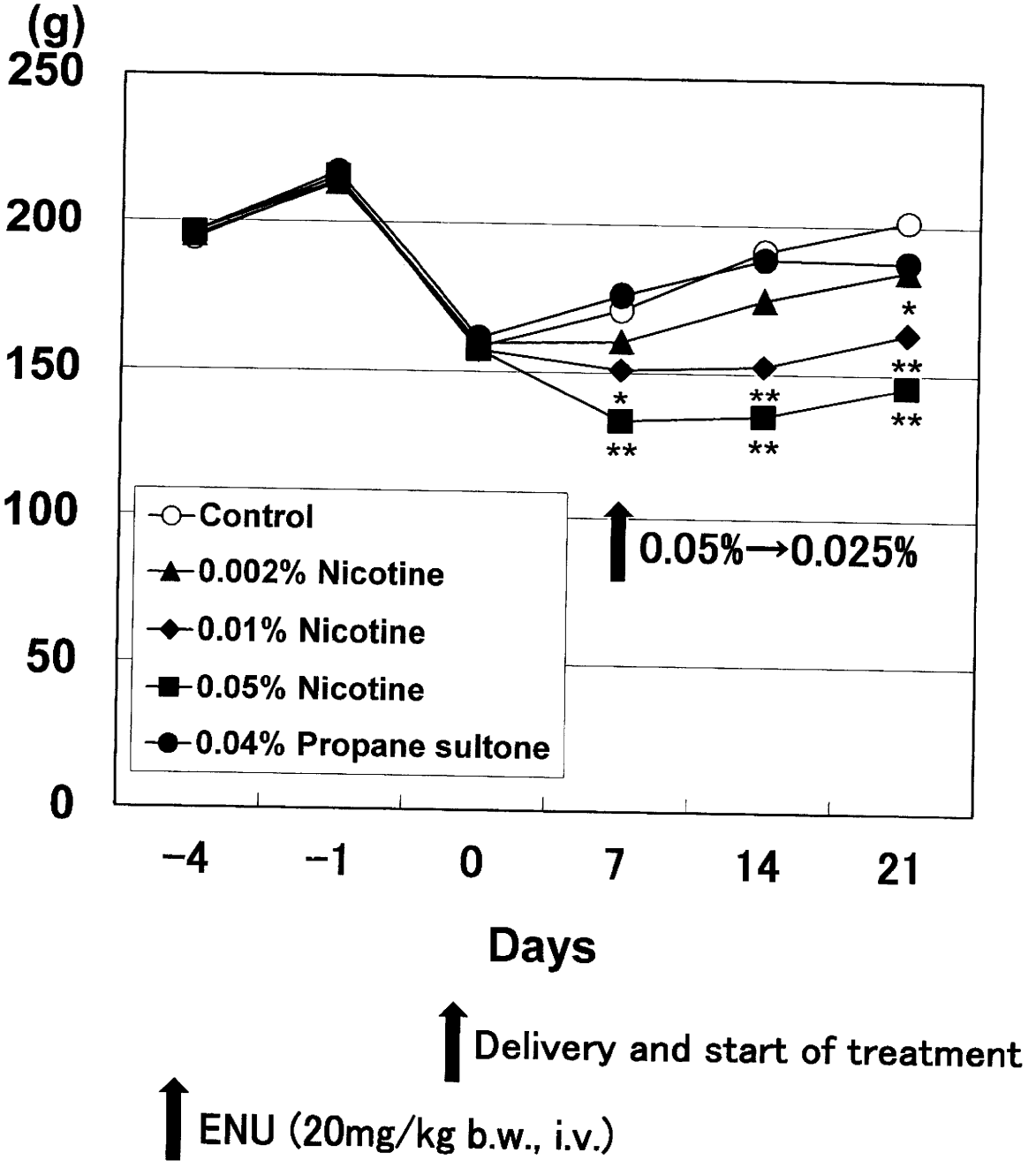

*,**:p<0.05 or 0.01 vs Control

Figure 8. Body weight curves of dams treated with nicotine or propane sultone for 3 weeks after ENU administration

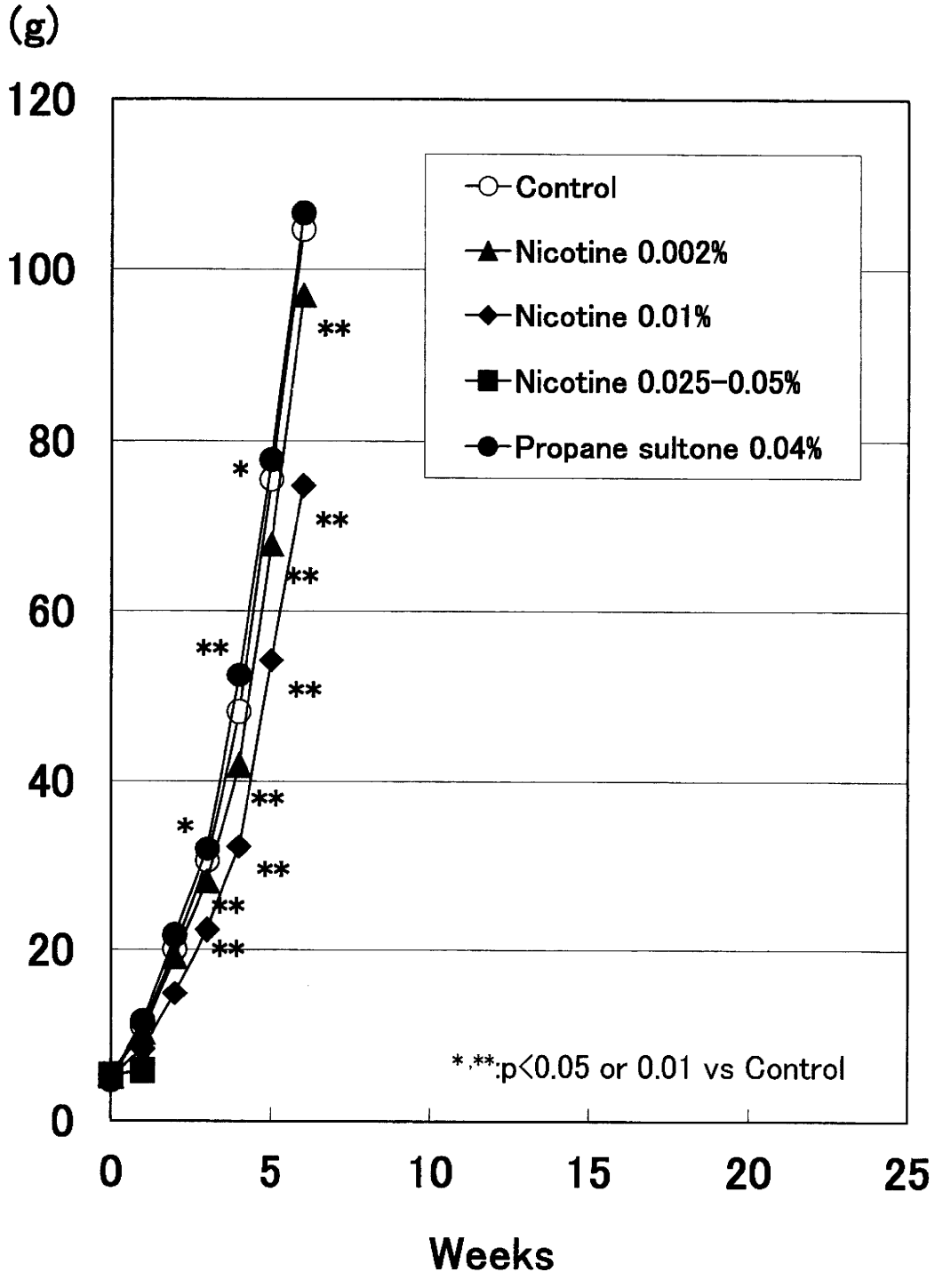

Figure 9. Body weight curves of offspring (male) treated with nicotine or propane sultone for 6 weeks

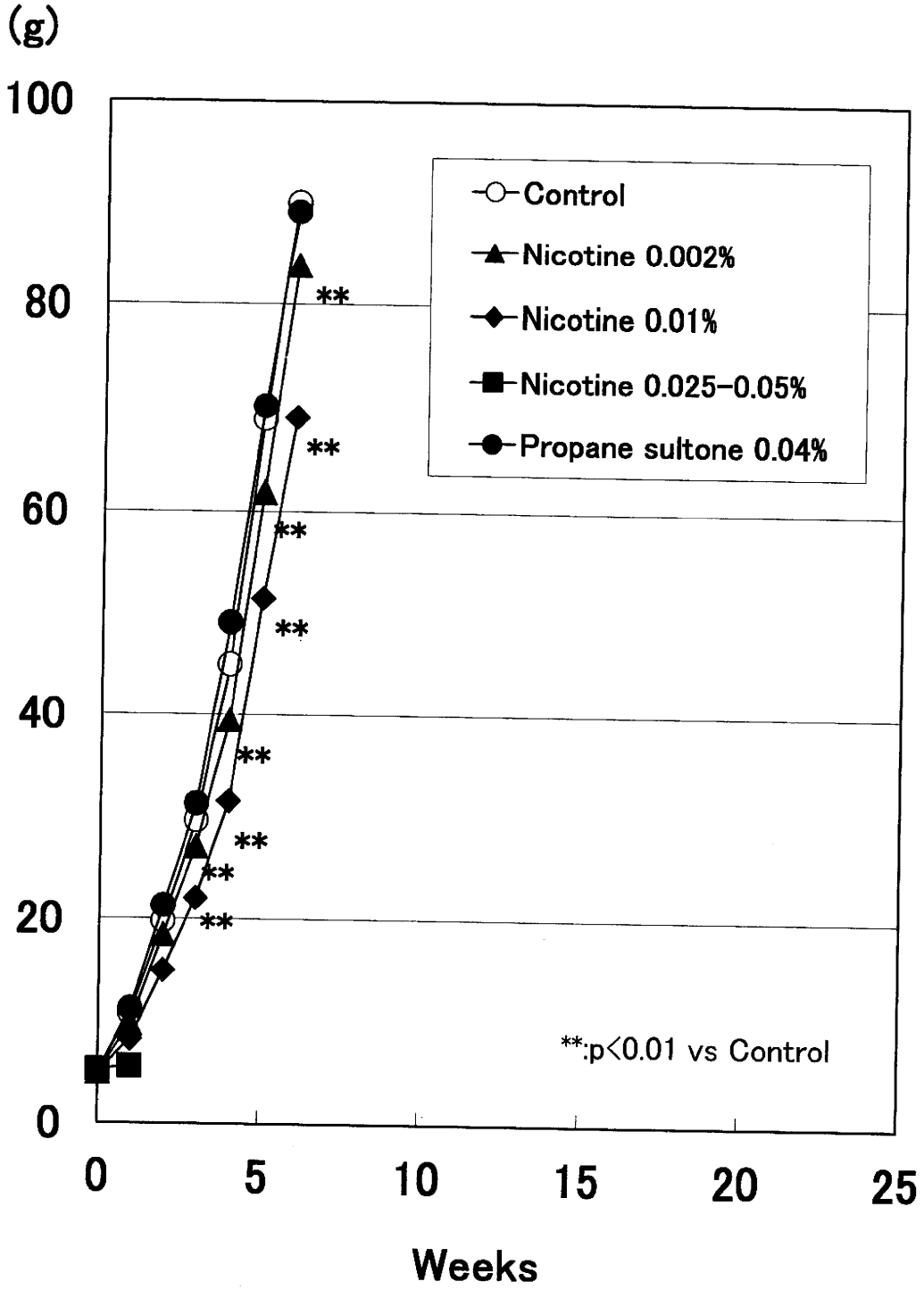

Figure 10. Body weight curves of offspring (female) treated with nicotine or propane sultone for 6 weeks

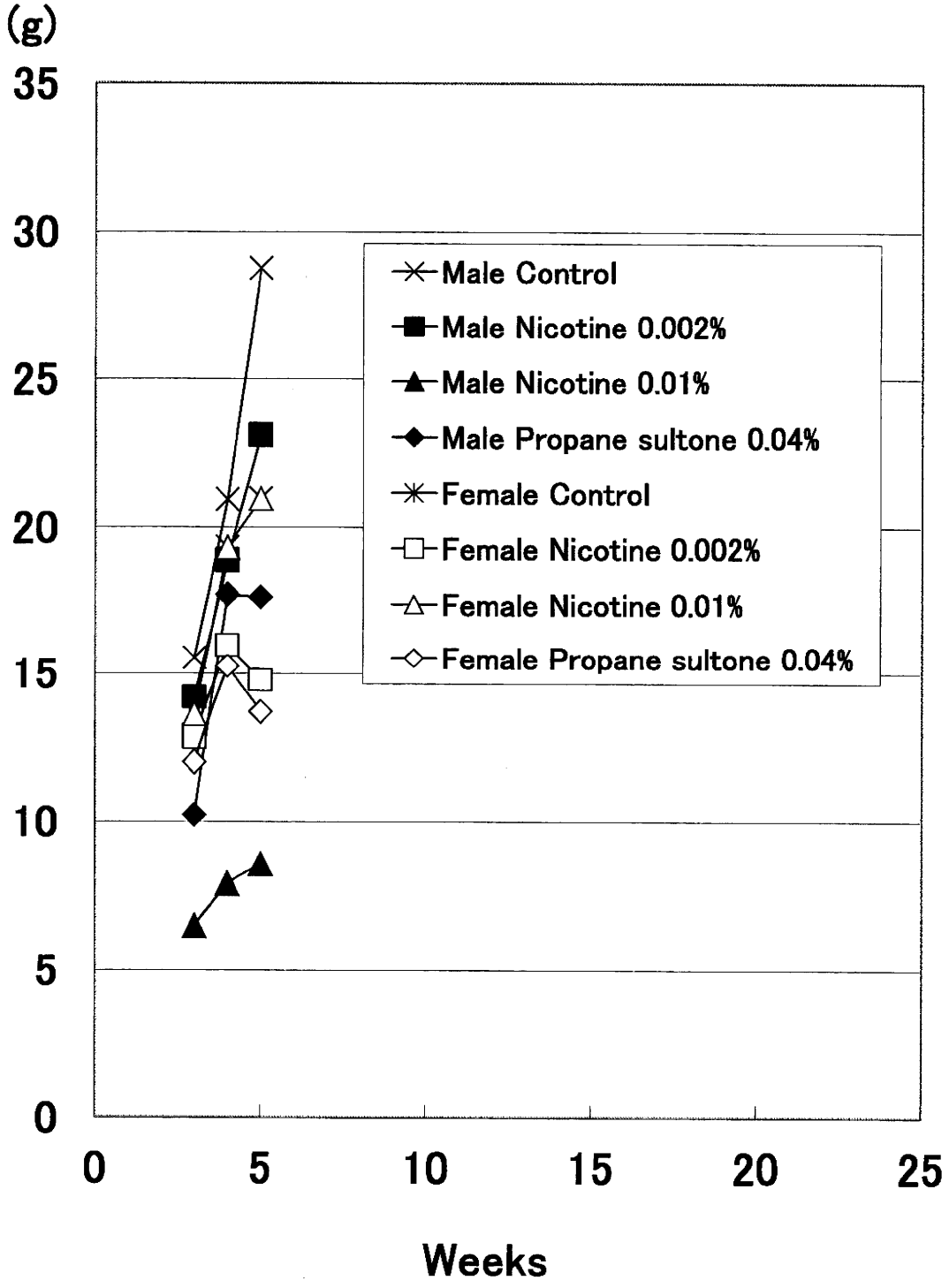

Figure 11. Food consumption of offspring treated with nicotine or propane sultone for 6 weeks

別添５

研究成果の刊行に関する一覧表レイアウト

書籍

著者氏名	論文タイトル名	書籍全体の編集者名	書　籍　名	出版社名	出版地	出版年	ページ
該当なし。							

雑誌

発表者氏名	論文タイトル名	発表誌名	巻号	ページ	出版年
Saegusa, Y., Shibutani, M., et al.	Gene expression profiling and cellular distribution of molecules with altered expression in the hippocampal CA1 region after developmental exposure to anti-thyroid agents in rats	J.Vet. Med. Sci.	72(2)	187-195	2010
Saegusa, Y., Shibutani, M., et al.	Sustained production of Reelin-expressing interneurons in the hippocampal dentate hilus after developmental exposure to anti-thyroid agents in rats	Reprod. Toxicol.	29(4)	407-414	2010
Ohishi, T., Shibutani, M., et al.	No effect of sustained systemic growth retardation on the distribution of Reelin-expressing interneurons in the neuron-producing hippocampal dentate gyrus in rats	Reprod. Toxicol.	30(4)	591-599	2010
Fujimoto, H., Shibutani, M., et al.	Impaired oligodendroglial development by decabromodiphenyl ether in rat offspring after maternal exposure from mid-gestation through lactation	Reprod. Toxicol.	31(1)	86-94	2011
Ogawa, B., Shibutani, M., et al.	Disruptive neuronal development by acrylamide in the hippocampal dentate hilus after developmental exposure in rats	Arch. Toxicol.		(in press)	
Takahashi, M., Shibutani, M., et al.	Life stage-related differences in susceptibility to acrylamide-induced neural and testicular toxicity	Arch. Toxicol.		(in press)	
Kuzumaki, N., Suzuki T., Narita, M. et al.	Hippocampal epigenetic modification at the brain-derived neurotrophic factor gene induced by an enriched environment	Hippocampus	21(2)	127-132	2011
Kuzumaki, N., Suzuki T., Narita, M. et al.	Hippocampal epigenetic modification at the doublecortin gene is involved in the impairment of neurogenesis with aging	Synapse	64(8)	611-616	2010
Kuzumaki, N., Suzuki T., Narita, M. et al.	Enhanced IL-1β production in response to the activation of hippocampal glial cells impairs neurogenesis in aged mice	Synapse	64(9)	721-728	2010

Hachisuka, A., Shibutani, M., Teshima, R. et al.	Effects of perinatal exposure to the brominated flame-retardant hexabromocyclododecane (HBCD) on the developing immune system in rats	Kokuritsu Iyakuhin Shokuhin Eisei Kenkyusho Hokoku	128	58-64	2010
Watanabe, W., Shimizu, T., et al.	Effects of tetrabromobisphenol A, a brominated flame retardant, on the immune response to respiratory syncytial virus infection in mice	Int.Immunopharmacol.	10(4)	393-397	2010
Watanabe, W., Shimizu, T., et al.	Functional disorder of primary immunity responding to respiratory syncytial virus infection in offspring mice exposed to a flame retardant, decabrominated diphenyl ether, perinatally	J. Med. Virol.	82(6)	1075-1082	2010

研究成果の刊行物・別刷

FULL PAPER *Pathology*

Gene Expression Profiling and Cellular Distribution of Molecules with Altered Expression in the Hippocampal CA1 Region after Developmental Exposure to Anti-Thyroid Agents in Rats

Yukie SAEGUSA[1,2], Gye-Hyeong WOO[3], Hitoshi FUJIMOTO[3], Kaoru INOUE[3], Miwa TAKAHASHI[3], Masao HIROSE[3,4], Katsuhide IGARASHI[5], Jun KANNO[5], Kunitoshi MITSUMORI[1], Akiyoshi NISHIKAWA[3] and Makoto SHIBUTANI[1]*

[1]*Laboratory of Veterinary Pathology, Tokyo University of Agriculture and Technology, 3–5–8 Saiwai-cho, Fuchu-shi, Tokyo 183–8509,* [2]*Pathogenetic Veterinary Science, United Graduate School of Veterinary Sciences, Gifu University, 1–1 Yanagido, Gifu-shi, Gifu 501–1193,* [3]*Division of Pathology and* [5]*Division of Molecular Toxicology, National Institute of Health Sciences, 1–18–1 Kamiyoga, Setagaya-ku, Tokyo 158–8501 and* [4]*Food Safety Commission, Akasaka Park Bld. 22nd F., 5–2–20 Akasaka, Minato-ku, Tokyo 100–8989, Japan*

(Received 6 September 2009/Accepted 8 Octoberr 2009/Published online in J-STAGE 27 November 2009)

ABSTRACT. To determine whether developmental hypothyroidism causes permanent disruption of neuronal development, we first performed a global gene expression profiling study targeting hippocampal CA1 neurons in male rats at the end of maternal exposure to anti-thyroid agents on weaning (postnatal day 20). As a result, genes associated with nervous system development, zinc ion binding, apoptosis and cell adhesion were commonly up- or down-regulated. Genes related to calcium ion binding were up-regulated and those for myelination were often down-regulated. We, then, examined immunohistochemical cellular distribution of Ephrin type A receptor 5 (EphA5) and Tachykinin receptor (Tacr)-3, those selected based on the gene expression profiles, in the hippocampal formation at the adult stage (11-week-old) as well as at the end of exposure. At weaning, both EphA5- and Tacr3-immunoreactive cells with strong intensities appeared in the pyramidal cell layer or stratum oriens of the hippocampal CA1 region. Although the magnitude of the change was decreased at the adult stage, Tacr3 in the CA1 region showed a sustained increase in expressing cells until the adult stage after developmental hypothyroidism. On the other hand, EphA5-expressing cells did not show sustained increase at the adult stage. The results suggest that developmental hypothyroidism caused sustained neuronal expression of Tacr3 in the hippocampal CA1 region, probably reflecting a neuroprotective mechanism for mismigration.

KEY WORDS: developmental hypothyroidism, EphA5, hippocampal CA1 region, Tacr3.

J. Vet. Med. Sci. 72(2): 187–195, 2010

Thyroid hormones are essential for normal fetal and neonatal brain development. They control neuronal and glial proliferation in definitive brain regions and regulate neural migration and differentiation [12, 18, 21]. In humans, maternal hypothyroxinemia, early in pregnancy, may have adverse effects on fetal brain development and importantly, even mild-moderate hypothyroxinemia may result in suboptimal neurodevelopment [4]. These results may increase the concern of thyroid hormone-disrupting chemicals in the environment.

Experimentally, developmental hypothyroidism leads to growth retardation, neurological defects and impaired performance on a variety of behavioral learning actions [1, 2]. Rat offspring exposed maternally to anti-thyroid agents such as 6-propyl-2-thiouracil (PTU) show brain retardation, with impaired neuronal migration and white matter hypoplasia involving limited axonal myelination and oligodendrocytic accumulation [6, 8, 21]. The outcome of this type of brain retardation is permanent and is accompanied by apparent structural and functional abnormalities. However, it is still unclear whether the molecular aberrations remain in the retarded brain after maturation.

Histological lesion-specific gene expression profiling provides valuable information on the mechanisms underlying lesion development. We have established molecular analysis methods for DNA, RNA and proteins in paraffin-embedded small tissue specimens utilizing an organic solvent-based fixative, methacarn, with high performance close to that achieved with unfixed frozen tissue specimens [22, 26, 27]. We have previously applied these techniques to analyze global gene expression changes in microdissected lesions [23, 28].

Hippocampal CA1 region is a well-known target of developmental hypothyroidism [8], and we, in our recent study, detected a distribution variability of hippocampal CA1 pyramidal neurons reflecting mismigration in rat offspring at the adult stage after developmental exposure to anti-thyroid agents [24]. The present study was performed to determine whether developmental hypothyroidism triggers sustained aberrations in neuronal development associated with neuronal mismigration until the adult stage. For this purpose, we first performed a global gene expression profiling of the CA1-pyramidal cell layer in rat offspring at the end of developmental exposure to anti-thyroid agents. To distinguish chemical-specific expression changes from hypothyroidism-linked ones, two different anti-thyroid

* CORRESPONDENCE TO: SHIBUTANI, M., Laboratory of Veterinary Pathology, Tokyo University of Agriculture and Technology, 3–5–8 Saiwai-cho, Fuchu-shi, Tokyo 183–8509, Japan.
e-mail: mshibuta@cc.tuat.ac.jp

agents, PTU and 2-mercapto-1-methylimidazole (MMI), were used, and dose-related responses were also examined with PTU. To extract the neuronal cell layer-specific gene expression profile, microdissection technique was applied for microarray analysis. Based on the expression profiles obtained, cellular localization of the molecules showing altered expression were then immunohistochemically examined in the hippocampus at the adult stage as well as at the end of the developmental exposure.

MATERIALS AND METHODS

Chemicals and animals: 6-propyl-2-thiouracil (PTU; CAS No. 51–52–5) and methimazole (2-mercapto-1-methylimidazole: MMI; CAS No. 60–56–0) were obtained from Sigma Chemical Co. (St. Louis, MO, U.S.A.). Pregnant Crj:CD®(SD)IGS rats were purchased from Charles River Japan Inc. (Yokohama, Japan) at gestation day (GD) 3 (appearance of vaginal plugs was designated as GD 0). Animals were housed individually in polycarbonate cages with wood chip bedding, maintained in an air-conditioned animal room (temperature: 24 ± 1°C; relative humidity: 55 ± 5%) with a 12-hr light/dark cycle and allowed *ad libitum* access to food and tap water. A soy-free diet (Oriental Yeast Co., Ltd., Tokyo, Japan) was chosen as the basal diet for the maternal animals to eliminate possible phytoestrogen effects [10], and water was given *ad libitum* throughout the experimental period including the 1-week acclimation period.

Animal experiments: The animal experiments were identical to those in a previous study [24]. In brief, maternal animals were randomly divided into four groups including untreated controls. Eight dams per group were treated with 3 or 12 ppm of PTU or 200 ppm of MMI in the drinking water from GD 10 to postnatal day (PND) 20 (PND 0: the day of delivery). On PND 2, the litters were culled randomly, leaving four male and four female offspring. On PND 20, 20 male and 20 female offspring (at least one male and one female per dam) per group were subjected to prepubertal necropsy [13, 24].

The remaining animals were maintained until postnatal week (PNW) 11. All offspring consumed the CRF-1 basal diet and tap water *ad libitum* from PND 21 onwards. At PNW 11, all pups were subjected to adult stage necropsy [13, 24].

All animals used in the present study were weighed and sacrificed by exsanguination from the abdominal aorta under deep anesthesia. These protocols were reviewed in terms of animal welfare and approved by the Animal Care and Use Committee of the National Institute of Health Sciences, Japan.

Preparation of tissue specimens and microdissection: For microarray and subsequent real-time RT-PCR analyses, the whole brain of male offspring was removed at prepubertal necropsy on PND 20 (n=4/group) and was fixed with methacarn solution for 2 hr at 4°C [22]. Coronal brain slices taken at the position of –3.5 mm from the bregma were dehydrated and embedded in paraffin. The embedded tissue blocks were stored at 4°C until tissue sectioning for microdissection [9].

For microdissection, 4-μm-thick sections between ten 20 μm-thick serial sections were prepared. The 4 μm-thick sections were stained with hematoxylin and eosin for confirmation of anatomical orientation of the hippocampal substructure to aid microdissection. The 20 μm-thick sections were mounted onto PEN-foil film (Leica Microsystems GmbH, Welzlar, Germany) overlaid on glass slides, dried in an incubator overnight at 37°C, and then stained using an LCM staining kit (Ambion, Inc., Austin, TX, U.S.A.). Bilateral sides of the hippocampal CA1 pyramidal cell layer in the sections were subjected to laser microbeam microdissection (Leica Microsystems GmbH) (Fig. 1). Twenty sections from each animal were used for microdissection, and the bilateral microdissected samples were collected and stored in separate 1.5-m*l* sample tubes at –80°C until the extraction of total RNA.

RNA preparation, amplification and microarray analysis: Total RNA extraction from hippocampal CA1 samples, quantitation of the RNA yield, and amplification of RNA samples were performed using previously described methods [9, 28].

For microarray analysis, second-round-amplified biotin-labeled antisense RNAs were subjected to hybridization with a GeneChip® Rat Genome 230 2.0 Array (Affymetrix, Inc., Santa Clara, CA, U.S.A.), as previously described [28].

The selection of genes and normalization of the expression data were performed using GeneSpring® software (ver7.2, Silicon Genetics, Redwood City, CA, U.S.A.). Per chip normalization was performed according to a previously described method [28]. Genes showing signals judged to be "absent" in all eight samples of untreated controls and in the anti-thyroid agent-exposed group were excluded. Genes

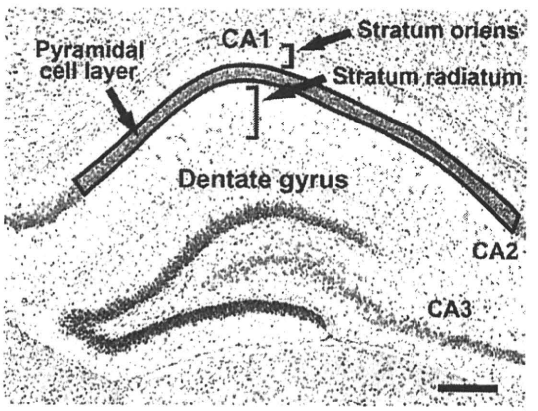

Fig. 1. Overview of the hippocampal formation of a male rat at postnatal day 20 stained with hematoxylin and eosin. Bar=200 μm. The CA1 pyramidal cell layer, enclosed by a solid line, was microdissected for the microarray and subsequent real-time RT-PCR analyses. The number of cells immunoreactive for the candidate molecules in this area was normalized for the length of CA1 used.

showing expression changes with differences of at least twofold in magnitude from the untreated controls were selected, and the "presence" signal in more than 3/4 of samples in each group showing higher expression values were selected. Genes showing altered expression in common in the anti-thyroid agent-exposed groups were also selected.

Real-time RT-PCR: Quantitative real-time RT-PCR was performed to confirm the expression values obtained with microarrays using an ABI Prism 7000 Sequence Detection System (Applied Biosystems Japan, Tokyo, Japan). Genes those showing altered expression (≥2-fold, ≤0.5-fold) in common in the anti-thyroid agent-exposed groups as compared with untreated control offspring were randomly selected, irrespective of the presence or absence of statistically significant difference. As a result, the following seven genes (four up-regulated and three down-regulated) with known function were selected as targets: Tachykinin receptor 3 (*Tacr3*), Calbindin 1, Slit homolog 2 (Drosophila) and Pleomorphic adenoma gene-like 1 (*Plagl1*) as up-regulated examples, and Myelin-associated oligodendrocytic basic protein (*Mobp*), Endothelial differentiation, sphingolipid G-protein-coupled receptor, 8 and CCAAT/enhancer binding protein as down-regulated. RT was performed using first-round antisense RNAs prepared for microarray analysis. For real-time PCR analysis of the genes selected, ABI Assays-on-Demand™ TaqMan® probe and primer sets from Applied Biosystems (available at https://products.appliedbiosystems.com/ab/en/US/adirect/ab?cmd=catNavigate2&catID=601267)(n=4/group) were used. For quantification of the expression data, a standard curve method was applied. The expression values were normalized to two housekeeping genes, Glyceraldehyde 3-phosphate dehydrogenase and Hypoxanthine-guanine phosphoribosyltransferase.

Immunohistochemistry: To evaluate the immunohistochemical distribution of the molecules selected by microarray analysis, the brains of male pups obtained at PND 20 or PNW 11 were fixed in Bouin's solution at room temperature overnight. Six animals were used as untreated controls, six for 200 ppm MMI, eight for 3 ppm PTU, and nine for 12 ppm PTU on PND 20. On PNW 11, 10 animals were used as untreated controls and 10 for 200 ppm MMI, nine for 3 ppm PTU, and six for 12 ppm PTU.

Immunohistochemistry was performed on the brain tissue sections of PND 20 and PNW 11 animals with antibodies against Ephrin type A receptor 5 (EphA5; rabbit IgG, 1:50; Abcam, Cambridge, U.K.) and Tacr3 (rabbit polyclonal antibody, 1:3,000, Novus Biologicals, Inc., Littleton, CO, U.S.A.), which were incubated with the tissue sections overnight at 4°C. Antigen retrieval treatment was not performed for these antigens. Immunodetection was carried out using a VECTASTAIN® Elite ABC kit (Vector Laboratories Inc., Burlingame, CA, U.S.A.) with 3,3'-diaminobenzidine/H_2O_2 as the chromogen, as previously described [23]. The sections were then counterstained with hematoxylin and coverslipped for microscopic examination.

With regard to EphA5, *Efna5*, a gene encoding the representative ligand for this receptor molecule [5], was found to be up-regulated (≥2-fold) by microarray analysis in all of the groups exposed to anti-thyroid agents in the present study (Table 1). Because distribution of EphA5 has been confirmed in the pyramidal cells of the hippocampal CA1 region at both developmental and adult stages in mice and at adult stage in humans [3, 17], we selected this molecule to examine distribution changes in the present study. Tacr3 was also up-regulated in all of the MMI and PTU groups by microarray analysis and real-time RT-PCR in the present study (Table 1). Expression of Tacr3 in the hippocampal CA1 pyramidal neurons has also been confirmed in rats [11], and therefore, we also selected this molecule for examination in the expression changes in the present study.

Morphometry of immunolocalized cells and apoptotic cells: EphA5- or Tacr3-immunoreactive cells distributed in the pyramidal cell layer or stratum oriens of the hippocampal CA1 region were bilaterally counted and normalized to the number in the length of the CA1 region measured (Fig. 1). Tacr3-immunoreactive cells in the subgranular zone of the dentate gyrus were also bilaterally counted and normalized for the number in the length of the granular zone measured. For quantitative measurement of each immunoreactive cellular component, digital photomicrographs at 100-fold magnification were taken using a BX51 microscope (Olympus Optical Co., Ltd., Tokyo, Japan) attached to a DP70 Digital Camera System (Olympus Optical Co., Ltd.), and quantitative measurements were performed using the WinROOF image analysis software package (version 5.7, Mitani Corp., Fukui, Japan).

Statistical analysis: Numerical data of the number of immunoreactive cells were assessed using Student's *t*-test to compare the untreated controls with each of the anti-thyroid agent-exposed groups when the variance was homogenous among the groups using a test for equal variance. If a significant difference in variance was observed, Aspin-Welch's *t*-test was used instead. The data for gene expression levels from real-time RT-PCR analysis were analyzed by the Kruskal-Wallis test, followed by Bartlett's test. When statistically significant differences were indicated, Dunnett's multiple test was used for comparisons with the untreated controls. For the microarray data, statistical analysis was performed with GeneSpring® software, and the significance of gene expression changes was analyzed by Student's *t*-test or ANOVA between the untreated controls and each of the anti-thyroid agent-exposed groups.

RESULTS

Microarray analysis: Figure 2 shows the Venn diagram of genes showing altered expression in the microdissected CA1 pyramidal neurons in the exposure groups in combination or individually in each exposure group. Many genes were found to be up- or down-regulated in common in two of the three groups. The numbers of genes classified into common categories between the groups or individually in each group were similar in terms of up- and down-regulated genes. The number of genes showing up- or down-regula-

Table 1. List of representative genes showing up- or down-regulation common to 2-mercapto-1-methylimidazole (MMI), 3 and 12 ppm 6-propyl-2-thiouracil (PTU) (≥2-fold, ≤0.5-fold)

Gene function	Accession No.	Gene title	Symbol	MMI	3 ppm PTU	12 ppm PTU
Up-regulated genes (of 119 genes in total)						
Nervous system development	AI101660	Slit homolog 2 (Drosophila)	Slit2	3.04	2.62	7.08
Nervous system development	NM_024358.1	Notch gene homolog 2 (Drosophila)	Notch2	2.52	2.01	2.02
Nervous system development	AW527295	Ephrin A5	Efna5	3.12	3.46	4.31
Nervous system development	NM_053465.1	Fucosyltransferase 9	Fut9	2.13	6.75	2.11
Nervous system development	BE106256	Sparc/osteonectin, cwcv and kazal-like domains proteoglycan 1	Spock1	3.22	3.13	2.15
Calcium ion binding	X04280.1	Calbindin 1	Calb1	4.48	4.85	9.00
Calcium ion binding	BM386119	UDP-N-acetyl-alpha-D-galactosamine:polypeptide N-acetylgalactosaminyltransferase 3 (GalNAc-T3)	Galnt3	2.43	2.30	2.63
Calcium ion binding	BI279663	Desmocollin 2	Dsc2	2.82	2.04	5.62
Calcium ion binding	AI105369	Calmodulin-like 4	Calml4	3.40	2.25	5.59
Zinc ion binding	BE098686	Similar to Tnf receptor-associated factor 1	LOC687813	3.10	2.04	2.78
Zinc ion binding	BF562032	RAN binding protein 2	Ranbp2	3.49	2.67	2.78
Zinc ion binding	BF397925	ADAMTS-like 1	Adamtsl1	6.22	2.55	7.63
Zinc ion binding	BF395606	Splicing factor, arginine/serine-rich 7	Sfrs7	4.93	2.06	2.90
Apoptosis	NM_012760.1	Pleomorphic adenoma gene-like 1	Plagl1	3.10	4.28	6.86
Apoptosis	NM_057130.1	Harakiri, BCL2 interacting protein (contains only BH3 domain)	Hrk	2.63	2.73	3.18
Cell Adhesion	AA850909	Poliovirus receptor-related 2	Pvrl2	4.74	2.46	2.61
Cell Adhesion	AA819731	Hyaluronan and proteoglycan link protein 4	Hapln4	4.13	6.67	3.46
Cell Adhesion	BI287851	Collagen, type VI, alpha 2	Col6a2	3.45	2.19	5.12
Ion channel activity	AA851939	FXYD domain-containing ion transport regulator 6	Fxyd6	4.73	2.61	7.85
Other	NM_017053.1	Tachykinin receptor 3	Tacr3	7.32	6.19	12.49
Down-regulated genes (of 97 genes in total)						
Nervous system development	NM_031018.1	Activating transcription factor 2	Atf2	0.41	0.36	0.36
Neuron migration	BF390065	Roundabout homolog 3 (Drosophila)	Robo3	0.06	0.31	0.04
Neuron differentiation	AF115249.1	Endothelial differentiation, sphingolipid G-protein-coupled receptor, 8	Edg8	0.40	0.06	0.08
Neuron differentiation	NM_024125.1	CCAAT/enhancer binding protein (C/EBP), beta	Cebpb	0.31	0.43	0.26
Myelination	X89638.1	Myelin-associated oligodendrocytic basic protein	Mobp	0.35	0.18	0.12
Myelination	NM_017190.1	Myelin-associated glycoprotein	Mag	0.47	0.36	0.29
Myelination	NM_022668.1	Myelin oligodendrocyte glycoprotein	Mog	0.44	0.32	0.19
Myelination	NM_012798.1	Mal, T-cell differentiation protein	Mal	0.37	0.28	0.28
Myelination	AA945178	Signal recognition particle receptor, B subunit transferrin	Srprb Tf	0.33	0.27	0.15
Zinc ion binding	NM_012566.1	Growth factor independent 1 transcription repressor	Gfi1	0.20	0.44	0.41
Zinc ion binding	AW529624	Zinc finger protein 91	Zfp91	0.33	0.32	0.38
Actin binding	AW522439	Ermin, ERM-like protein	Ermn	0.43	0.42	0.28
Apoptosis	BG377720	Solute carrier family 5 (sodium/glucose cotransporter), member 11	Slc5a11	0.25	0.19	0.19
Apoptosis	U21955.1	Eph receptor A	Epha7	0.34	0.48	0.18
Cell Adhesion	BM391100	Mucin 4, cell surface associated	Muc4	0.43	0.36	0.27
Other	AW435010	Protein tyrosine phosphatase, non-receptor type 3	Ptpn3	0.38	0.46	0.36
Other	AF312319.1	gamma-aminobutyric acid (GABA) B receptor 1	Gabbr1	0.33	0.41	0.39
Other	NM_053936.1	Endothelial differentiation, lysophosphatidic acid G-protein-coupled receptor, 2	Edg2	0.47	0.31	0.31

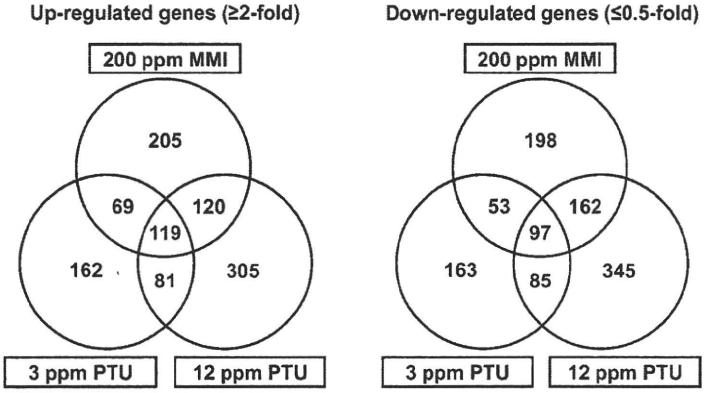

Fig. 2. Venn diagram of gene populations showing altered expression in the hippocampal CA1 pyramidal cell layer at postnatal day 20 in response to maternal exposure to propylthiouracil and/or 2-mercapto-1-methylimidazole compared with the untreated controls. (Left) Up-regulated genes (≥2-fold). (Right) Down-regulated genes (≤0.5-fold). Abbreviations: MMI, 2-mercapto-1-methylimidazole; PTU, 6-propyl-2-thiouracil.

Table 2. Validation of microarray data by real-time RT-PCR

Gene	200 ppm MMI			3 ppm PTU			12 ppm PTU		
	Microarray	Real-time RT-PCR normalized to		Microarray	Real-time RT-PCR normalized to		Microarray	Real-time RT-PCR normalized to	
		Hprt[a]	Gapdh[b]		Hprt	Gapdh		Hprt	Gapdh
Tacr3[c]	7.32 ± 2.21**	4.29 ± 1.27	4.08 ± 1.15*	6.19 ± 2.19**	3.46 ± 1.42	3.76 ± 1.51*	12.49 ± 1.56**	9.23 ± 3.00**	8.81 ± 1.60**
Calb1[d]	4.48 ± 0.66*	3.96 ± 0.74	3.67 ± 0.16	4.85 ± 2.53*	4.74 ± 2.48	4.93 ± 3.79	9.00 ± 1.85**	11.13 ± 2.13**	10.53 ± 3.26**
Slit2[e]	3.04 ± 0.79	2.83 ± 0.90	4.08 ± 1.15*	2.62 ± 1.16	1.33 ± 0.67	3.67 ± 1.51*	7.08 ± 2.15**	4.72 ± 2.57**	8.81 ± 1.60**
Plgl1[f]	3.10 ± 1.57	12.67 ± 5.00	11.5 ± 7.50	4.28 ± 2.88	18.33 ± 6.00	19.00 ± 9.00*	6.86 ± 2.85**	30.67 ± 5.33**	27.00 ± 8.00**
Mobp[g]	0.35 ± 0.15**	0.6 ± 0.22*	0.52 ± 0.16**	0.18 ± 0.07**	0.24 ± 0.07**	0.24 ± 0.05**	0.12 ± 0.02**	0.18 ± 0.04**	0.16 ± 0.04**
Edg8[h]	0.40 ± 0.11*	0.49 ± 0.16*	0.43 ± 0.13*	0.06 ± 0.05**	0.29 ± 0.10**	0.28 ± 0.08**	0.08 ± 0.07**	0.21 ± 0.07**	0.18 ± 0.03**
Cebpb[i]	0.31 ± 0.06**	0.43 ± 0.04**	0.38 ± 0.06**	0.43 ± 0.18**	0.77 ± 0.07	0.76 ± 0.10	0.26 ± 0.04**	0.39 ± 0.16**	0.35 ± 0.22**

a) Hprt, Hypoxanthine-guanine phosphoribosyltransferase; b) Gapdh, Glyceraldehyde 3-phosphate dehydrogenase; c) Tacr3, Tachykinin receptor 3; d) Calb1, Calbindin 1; e) Slit2, Slit homolog 2 (Drosophila); f) Plgl1, Pleomorphic adenoma gene-like 1; g) Mobp, Myelin-associated oligodendrocytic basic protein; h) Edg8, Endothelial differentiation, sphingolipid G-protein-coupled receptor, 8; i) Cebpb, CCAAT/enhancer binding protein (C/EBP), beta.

Values are mean ± SD (n=4) relative to the expression level in the untreated controls. Real-time RT-PCR analysis of Hprt and Gapdh was performed in the analysis of each target gene.

*, **: Significantly different from the untreated controls at $P<0.05$ and $P<0.01$, respectively (Dunnett's multiple comparison test).

tion in response to 12 ppm PTU was approximately 2-fold higher than that with 3 ppm PTU. The number of genes showing up- or down-regulation in response to 200 ppm MMI was in between that elicited by 3 or 12 ppm PTU. One-hundred nineteen genes were up-regulated in common by MMI and PTU, with PTU showing up-regulation from 3 ppm. On the other hand, 97 genes showed down-regulation in all MMI and PTU groups. Representative genes showing up- or down-regulation in all three groups are shown in the Table 1. Among the genes listed, genes associated with nervous system development, zinc ion binding, apoptosis and cell adhesion were commonly up- or down-regulated. Genes related to calcium ion binding were found to be up-regulated and those for myelination were often down-regulated.

Real-time RT-PCR analysis: For confirmation of the microarray data, four genes that were up-regulated and three that were down-regulated in response to anti-thyroid agents were selected for mRNA expression analysis by real-time RT-PCR and the results are summarized in Table 2.

In all exposure groups, many of the expression changes were similar in the two analysis systems, except for much higher expression of *Plagl1* in all exposure groups by real-time RT-PCR as compared with findings from the microarray system.

Although we performed expression analysis of *Efna5* by real-time RT-PCR, expression values were rather low with great variability between samples, and therefore, reliable quantitative data could not be obtained (data not shown).

Immunolocalization of EphA5 and Tacr3 in the hippoc-